

Amplitude Instabilities of Transverse Traveling Waves in Lasers

Q. Feng, J. V. Moloney, and A. C. Newell

Department of Mathematics, University of Arizona, Tucson, Arizona 85721

(Received 20 May 1993)

A new class of amplitude instabilities severely restricts the stability domain of the transverse patterns in a laser that takes the form of a continuum of waves traveling transverse to the laser axis. Linear stability analyses and numerical solution of the laser equations reveal that one of the instabilities, which should be manifest in a broad range of contexts for which traveling waves are the preferred pattern, results in the death of the traveling wave and its replacement by a wave traveling in the opposite direction which exhibits novel transient and asymptotic behavior.

PACS numbers: 42.55.-f, 42.60.Mi, 47.20.Ky

The study of spatial structures in nonequilibrium systems has become increasingly popular. Recently, several studies have been devoted to patterns in the transverse section of lasers and have revealed interesting symmetry breaking process and complex spatial structures [1-3]. Because of fast time scales, lasers have many potential advantages over hydrodynamics for exploring complex spatiotemporal behavior in patterns [4].

In this Letter, we analyze the stability of traveling waves in the transverse section of a laser cavity [2,3]. These waves represent a natural state in the sense that for positive detuning $\Omega = \omega_a - \omega_{cav}$, the frequency difference between the atomic line frequency relevant to the lasing action and the frequency of the longitudinal cavity mode nearest to ω_a , the lasing threshold can be decreased by the excitation of a number of transverse traveling wave modes whose natural frequencies are closer to ω_a . There is therefore selective amplification of the various possible lasing configurations and this in turn leads to the formation of patterns in the output signal. The emerging transverse patterns may be one of a variety of plan forms: unidirectional traveling waves, standing waves, square standing waves, etc., depending on transverse boundary conditions. In the theoretically simplest situation, corresponding to periodic boundary conditions relevant to a case in which the lasing takes place in an annular region between two cylinders, the unidirectional traveling wave dominates [2,3]. Our purpose is to draw stability diagrams for these solutions. There are practical reasons for doing this. When stable, each cell or wave in the wave train acts as an individual laser whose output is *synchronized*. The borders of the stability domain correspond to various long (phase) or short (amplitude) wavelength instabilities [5]. The former (e.g., Eckhaus, zigzag, skew varicose) involve the growth of sideband modes with wave vectors and frequencies in the neighborhood of that of the underlying traveling wave. The latter (e.g., cross roll, knot, oscillatory skew varicose) are more difficult to identify as they involve the growth of modes whose wave vectors and frequencies are significantly different from that of the original traveling wave. The novel feature of this Letter is the identification of a new class of short wavelength instabilities which severely restrict the sta-

bility domain (in pump-parameter-wave-number space) of the traveling waves. One of these instabilities in particular is very dramatic and is readily triggered when the wave number selected by external conditions (e.g., by the presence of a nearby defect) is slightly greater than the critical wave number. The development of this instability is followed by our numerical simulation. It reverses the direction of the traveling wave and leads to an interesting transient state which in turn is Eckhaus unstable and evolves to a weakly turbulent state. We expect that the scenario described in this Letter is applicable in many other contexts such as convection in binary mixture fluids [6] and liquid crystals [7], each of which shows many of the symmetries and characteristics of the laser optics situation.

Our starting point is the Maxwell-Bloch equations governing the dynamics of a homogeneously broadened, single-longitudinal mode, unidirectional ring laser. In dimensionless form these equations read [3]

$$\begin{aligned} \partial_t A - ia\partial_x^2 A + \sigma A - \sigma P &= 0, \\ \partial_t P - rA + (1 + i\Omega)P &= -An, \\ \partial_t n + bn &= \text{Re}(AP^*), \end{aligned} \quad (1)$$

where A , P , and n are the appropriately scaled envelopes of the electric field, polarization, and inversion population of the two-level atom system, respectively. The dependence $e^{-i\omega_{cav}(t-z/c)}$ has been scaled out of the first two fields. The detuning, Ω , the electric field, and inversion decay rates, σ and b , are normalized to the polarization decay rate. The parameter r is proportional to the pumping and acts as the main control parameter analogous to the Rayleigh number in fluid convection [5]. a is the diffraction coefficient. In this Letter we will restrict ourself to the case of one transverse dimension (x), because the new instabilities are one dimensional (see below).

When r is increased, the nonlasing solution $(A, P, n) = 0$ loses stability and gives way to the lasing state, which takes the form of traveling waves in the transverse direction [2,3]:

$$A_{tw} = A_0 e^{i(kx - \omega t)}, \quad P_{tw} = P_0 e^{i(kx - \omega t)}, \quad n_{tw} = n_0, \quad (2)$$

where A_0 , P_0 , n_0 , and ω are given by

$$|A_0|^2 = b[r - r_0(k)], \quad n_0 = r - r_0(k),$$

$$\omega = \frac{ak^2 + \sigma\Omega}{1 + \sigma}, \quad P_0 = \frac{r_0(k)}{1 + i(\Omega - \omega)} A_0, \quad (3)$$

with the *neutral stability curve*

$$r_0(k) = 1 + (\Omega - ak^2)^2 / (1 + \sigma)^2. \quad (4)$$

For the given wave number k , the traveling wave solution exists if $r > r_0(k)$. Minimizing $r_0(k)$ with respect to k gives the lasing threshold $r_c = r_0(k_c)$ with critical wave number k_c and critical frequency $\omega_c = \omega(k_c)$. For the case of positive detuning $\Omega > 0$, which will be considered throughout this Letter, we have $k_c = \pm\sqrt{\Omega/a}$, $r_c = 1$, and $\omega_c = \Omega$, so that the frequency of the electric field is $\omega_{\text{cav}} + \omega_c = \omega_a$, the atomic line frequency. Therefore, by choosing the appropriate transverse structure, the laser can operate at the frequency natural to the medium and the constraints of the end mirrors are removed. They are replaced, of course, by the constraints of transverse boundaries. Here, however, in order to concentrate on what are the main new results, we will assume that, by virtue of an appropriate annular (and therefore periodic) geometry, they do not play an important role.

We study the stability of the traveling wave solution (2) by adding $(v_1 e^{isx} + v_2 e^{-isx}) e^{i(kx - \omega t)}$, $(v_3 e^{isx} + v_4 e^{-isx}) e^{i(kx - \omega t)}$, and $v_5 e^{isx} + v_5^* e^{-isx}$ to each of the fields A_{tw} , P_{tw} , and n_{tw} and linearizing the resulting system about the latter. We obtain $\partial_t \mathbf{v} = \mathcal{M}(k, r, s) \mathbf{v}$, where \mathcal{M} is 5×5 matrix and \mathbf{v} denotes the column vector $(v_1, v_2^*, v_3, v_4^*, v_5)^T$. The time dependence of \mathbf{v} is chosen to be $e^{\lambda t}$ and λ is determined as an eigenvalue of \mathcal{M} . This system is solved numerically. If for a given k and r there exists a modulation wave number s such that $\text{Re}[\lambda(k, r; s)] > 0$, the traveling wave represented by (k, r) is unstable; otherwise, it will be regarded as linearly stable.

In what follows, we draw the stability boundaries in the (r, k) plane (Busse balloon) and identify their nature. We state straightaway that an analysis of two-dimensional disturbances reveals only the expected: the zigzag instability will destabilize all traveling waves whose wave number k is less than k_c . We have chosen the following parameter set to display our results: $a = 0.01$, $\sigma = 1$, $\Omega = 0.3$, and $b = 0.1$. A range of parameters (e.g., $a = 0.01$, $\sigma = 0.7$, $\Omega = 0.3$, and $b = 0.01$) has been explored and similar behavior was found. Hence our laser may be regarded as in class B in the classification of Ref. [8], but with relative large electric-field decay rate which can be easily achieved in experiments.

Figure 1(a) shows the stability diagram. The near threshold regime and its local enlargement is shown in Fig. 1(b). The stable region of traveling wave solution is limited by the Eckhaus instability (dashed line) and new instabilities (solid and dotted lines) which we call *amplitude instabilities* because they involve the excitation of new modes with distinctly different wave numbers, i.e., s is finite. The ubiquitous and universal Eckhaus insta-

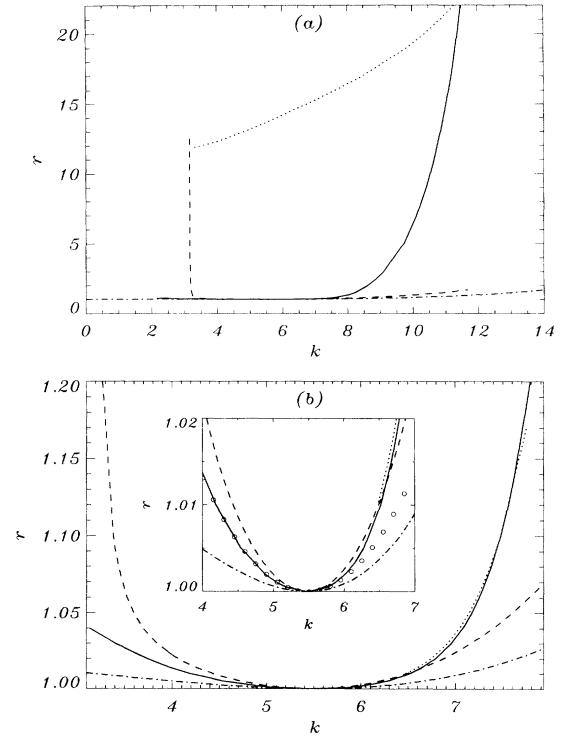


FIG. 1. Stability diagram in the (k, r) plane. The low- r part of (a) is enlarged in (b). Traveling waves are stable in the region enclosed by the solid, dotted, and dashed lines. Dash-dotted line: neutral curve; dashed line: Eckhaus stability limit. The solid line in (a) and (b), the dotted line in (a), and the dotted line in (b) represent, respectively, three different amplitude instabilities. The open circles in the inset of (b) mark the instability line obtained from amplitude equations. The stability diagram for negative k is a symmetric image with respect to the r axis.

bility [9] has already been identified for lasers [10]. The new instabilities are denoted by the solid line in Figs. 1(a) and 1(b), the dotted line in Fig. 1(a), and the dotted line in Fig. 1(b). Each sets in at values of the perturbation wave number s different from zero and with finite values of $\text{Im}(\lambda)$ which are of the same order of magnitude as frequencies of the traveling waves.

Figure 2 plots the largest $\text{Re}(\lambda)$ versus the perturbation wave number s in the neighborhood of (k, r) at which the amplitude instabilities set in. The curves consisting of diamonds (open and filled) are typical of the growth rate curves of instabilities of the waves whose (k, r) values are denoted by the dotted line in Fig. 1(a). The instability occurs for values of r far above threshold and the most unstable perturbation wave number s_m , corresponding to maximum growth, is typically of order k_c but varies along the stability border. The dotted and dashed lines are growth rate curves for another amplitude instability that occurs at the dotted line of Fig. 1(b). As (k, r) moves along this instability line towards the Eck-

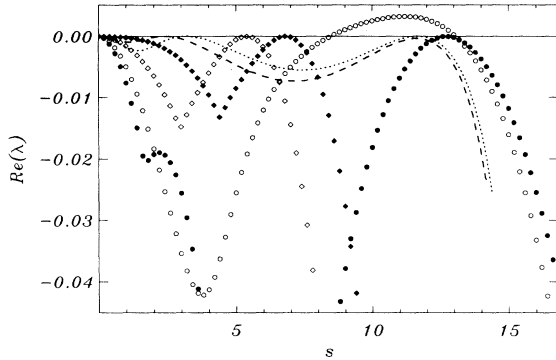


FIG. 2. The largest real part of eigenvalues (growth or decay rates) as functions of modulation wave number s for (k, r) on the amplitude-instability lines. Curves consisting of diamonds are for instability occurring on the dotted line in Fig. 1(a) (solid: $k = 3.5, r = 11.973$; open: $k = k_c = 5.477, r = 13.634$), circles for instability on the solid line in Figs. 1(a) and 1(b) (solid: $k = 10.655, r = 11$; open: $k = 9, r = 2.53$), dotted and dashed lines for instability on the dotted line in Fig. 1(b) (dotted: $k = 7.475, r = 1.1$; dashed: $7.142, r = 1.05$).

haus border, s_m approaches zero and the growth-rate curve merges into Eckhaus growth-rate curve.

The circles (open and filled) in Fig. 2 give typical growth-rate curves for the amplitude instability which sets in at the solid lines of Figs. 1(a) and 1(b). We have studied this instability in detail. Here the most excited mode is $s_m \gtrsim 2k_c$. Near threshold it lies in the Eckhaus unstable regime and one observes that the perturbation amplitudes v_2 and v_4 dominate v_1, v_3 , and v_5 and that $s_m \approx 2k_c, \text{Im}(\lambda) \approx 0$. So the instability gives rise to a left traveling wave with the wave number near $2k_c - k$. (The instability is analogous to the cross-roll instability [5] experienced by stationary convection rolls at large Prandtl number in which, as the wave number is increased, the pattern develops an instability to an orthogonal set of rolls with the wave number close to k_c .) We have confirmed this picture by looking at the interaction between oppositely traveling waves near threshold for which the amplitude equations are [2,3]

$$\tau_0(\partial_t \pm v_g \partial_x) A_{\pm} = \epsilon A_{\pm} + \xi_0^2(1 + ic_1) \partial_x^2 A_{\pm} - g(1 + ic_2)(|A_{\pm}|^2 + \beta |A_{\mp}|^2) A_{\pm}, \quad (5)$$

where $\tau_0 = (\sigma + 1)/\sigma$, $\epsilon = r - 1$, $v_g = 2ak_c/(\sigma + 1) = \xi_0$, $c_1 = (1 + \sigma)^2/4\sigma ak_c^2$, $g = 1/b$, and $\beta = 2$. A_+ and A_- are the amplitudes of right- and left-traveling waves, respectively,

$$(A, P, n) = \mathbf{U}[A_+ e^{i(k_c x - \omega_c t)} + A_- e^{-i(k_c x + \omega_c t)}]. \quad (6)$$

[$\mathbf{U} = (1, 1, 0)$ is the linear eigenvector.] From the amplitude equations one can solve for right-traveling wave solution $A_+ = \rho e^{i(qx - \nu t)}$ with $\rho = \sqrt{(\epsilon - \xi_0^2 q^2)/g}$ (note that the wave number is $k = k_c + q$), and then perturb it with small left-traveling wave $A_- \propto e^{\gamma t + ipx}$ (wave num-

ber $-k_c + p$). Stability requires $\max_p \text{Re}[\gamma(p)] < 0$, which is

$$(k - k_c)^2 = q^2 < \left(1 - \frac{1}{\beta}\right) \frac{\epsilon}{\xi_0^2} = \frac{1}{2} \left(\frac{\sigma + 1}{2ak_c}\right)^2 (r - 1). \quad (7)$$

The stability boundary is shown by the open circles in the inset of Fig. 1(b) and it agrees well with the numerical results for r close to $r_c = 1$. From (7) one sees that this instability happens only for $\beta > 1$, the regime in which traveling waves are preferred to standing waves. This means the interaction between right- and left-traveling waves must be strong enough for the instability to occur. In our case $\beta = 2$ and is parameter independent. The extension of the instability curve (7) to higher values of r is the solid line in Fig. 1.

The finite amplitude saturation of this instability is most interesting. Taking the traveling wave with $k = 9, r = 2.53$ as the initial state (the curve showing the growth rates of perturbation modes as a function of perturbation wave number s is given by the open circles in Fig. 2), we follow its evolution in Fig. 3. Figure 3(a) shows a dramatic transition from a right-traveling wave to a left-traveling wave. One can see that the wavelength of the left-going wave is not uniform in space [see also Fig. 3(b)]: there are large spatial intervals where it changes slowly. This slowly varying feature can be captured by the local wave number which is defined as gradient of the phase θ of the complex electric field envelope $A(x, t)$: $k_{\text{loc}} \equiv \partial_x \theta = \text{Im}(A^{-1} \partial_x A)$. Figure 3(b) illustrates evolution of the local wave number (left half) of the resulting left-traveling wave. On the right half the solid lines give the local amplitude $|A|$ at corresponding times and the dotted lines are obtained from $\sqrt{b[r - r_0(k_{\text{loc}})]}$, the formula for the amplitude of pure traveling waves [see Eq. (3)]. At time $t = 21000$ there is a narrow interval, in which the local wave number and amplitude change rapidly, embedded in a large interval where k_{loc} changes slowly, in fact, linearly, giving rise to an overall chirp in the phase, and where the local amplitude evaluated from k_{loc} agrees remarkably well with the exact amplitude. This indicates that in the slowly varying domain the phase is the only active variable and the amplitude is slaved to the phase. The narrow, fast varying region also travels to the left. As time goes on, it expands into the surrounding slowly varying domain and the slope of k_{loc} in the slowly varying domain decreases ($t = 38000$). As k_{loc} in the slowly varying domain becomes more and more uniform, one can expect that the Eckhaus instability will occur because the central wave number is in the Eckhaus unstable region (see Fig. 1). The oscillation in the local wave number and amplitude at positions away from the fast varying domain for $t = 50000$ appears to be generated by the Eckhaus instability. Eventually the system evolves into a weakly turbulent state ($t = 90000$) in the sense that the amplitude modulation is spatiotem-

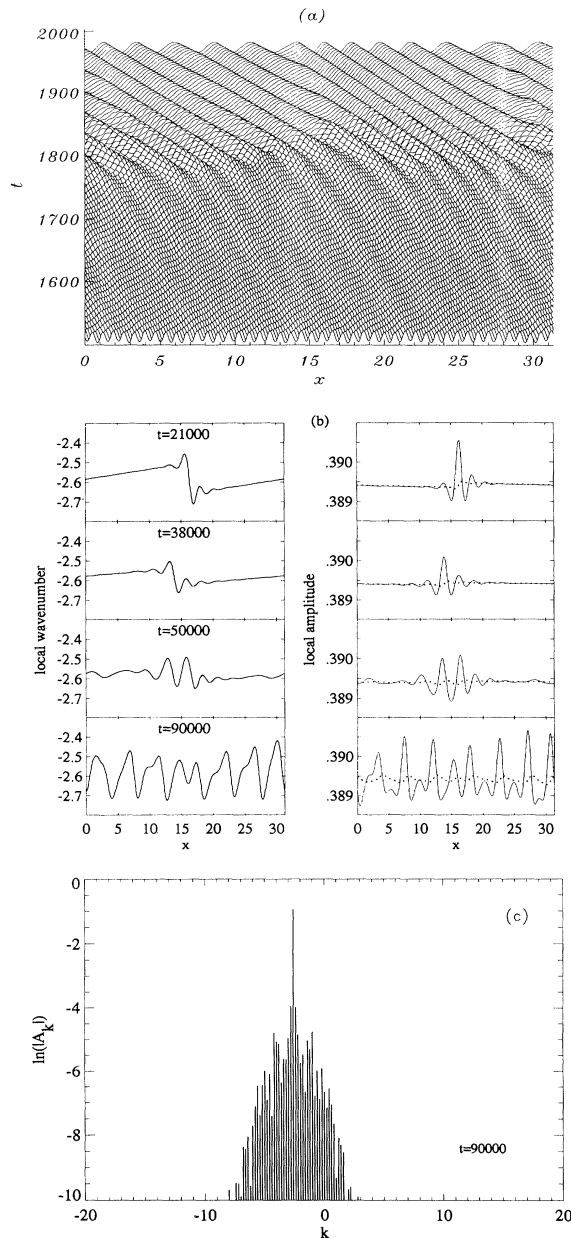


FIG. 3. Numerical simulation with unstable traveling wave of $k = 9, r = 2.53$ as initial state (the growth-rate curve is given by open circles in Fig. 2). (a) Transition from right-traveling wave to left-traveling wave [real part of the electric field vs (x, t)]. (b) Local wave number at different times (left half) and amplitude of the electric field (solid lines) at corresponding times (right half). The dotted lines are the local amplitude evaluated from the local wave number. (c) Spatiotemporal spectrum at $t = 90\,000$.

porally chaotic but very small. In this state the amplitude no longer follows the phase everywhere, as indicated by the discrepancy between solid and dotted lines for $t = 90\,000$, and is itself an active variable. We give in Fig. 3(c) the wave-number spectrum for this weakly turbulent state. It is dominated by a wave with wave number $k_f = -2.6$ which is close to the most unstable wave number, $k - s_m = 9 - 11.2 = -2.2$, of the initial wave. (In another run with double size of x domain, we obtained $k_f = -2.15$.)

Finally we mention that we have also carried out a numerical simulation of an Eckhaus unstable wave with wave number k_f and observed the direct transition to turbulent states very similar to the one described above.

The authors wish to thank the Arizona Center for Mathematical Sciences (ACMS) for support. ACMS is sponsored by AFOSR Contract No. F49620-86-C0130 with the University Research Initiative Program at the University of Arizona. Q.F. is grateful to R. Indik, P. Ru, and G. Harkness for many helpful discussions.

- [1] N. B. Abraham and W. J. Firth, *J. Opt. Soc. Am. B* **7**, 951 (1990), and references therein. For more recent references, see, e.g., R. López Ruiz, G. B. Mindlin, and C. Pérez García, *Phys. Rev. A* **47**, 500 (1993).
- [2] P. K. Jakobsen, J. V. Moloney, A. C. Newell, and R. Indik, *Phys. Rev. A* **45**, 8129 (1992).
- [3] A. C. Newell and J. V. Moloney, *Nonlinear Optics* (Addison-Wesley, Redwood City, CA, 1992).
- [4] M.C. Cross and P.C. Hohenberg, *Rev. Mod. Phys.* (to be published).
- [5] F. H. Busse, *Rep. Prog. Phys.* **41**, 28 (1978).
- [6] See, e.g., P. Kolodner, D. Bensimon, and C. M. Surko, *Phys. Rev. Lett.* **60**, 1723 (1988); P. Kolodner, *Phys. Rev. A* **46**, 6431 (1992).
- [7] Complex space-time behavior, including transition between oppositely traveling waves, has been observed in convection in nematic liquid crystals, see A. Joets and R. Ribotta, in *New Trends in Nonlinear Dynamics and Pattern Forming Phenomena: the Geometry of Nonequilibrium*, edited by P. Coulet and P. Huerre, NATO ASI, Ser. B2, Vol. 237 (Plenum, New York, 1990).
- [8] F. T. Arecchi, in *Instabilities and Chaos in Quantum Optics*, Springer Series in Synergetics Vol. 34, edited by F. T. Arecchi and R. G. Harrison (Springer-Verlag, Berlin, 1987).
- [9] W. Eckhaus, *Studies in Nonlinear Stability Theory* (Springer, New York, 1965); B. Janiaud, A. Pumir, D. Bensimon, V. Croquette, H. Richter, and L. Kramer, *Physica (Amsterdam)* **55D**, 269 (1992).
- [10] J. Lega, P. K. Jakobsen, J. V. Moloney, and A. C. Newell (to be published).